JPP Journal of Pharmacy and Pharmacology

JPP 2005, 57: 1529–1537

Received April 21, 2005
Accepted August 12, 2005
DOI 10.1211/jpp.57.12.0003
ISSN 0022-3573

Cefuroxime axetil solid dispersions prepared using solution enhanced dispersion by supercritical fluids

Seoung Wook Jun, Min-Soo Kim, Guk Hyun Jo, Sibeum Lee, Jong Soo Woo, Jeong-Sook Park and Sung-Joo Hwang

Abstract

Cefuroxime axetil (CA) solid dispersions with HPMC 2910/PVP K-30 were prepared using solution enhanced dispersion by supercritical fluids (SEDS) in an effort to increase the dissolution rate of poorly water-soluble drugs. Their physicochemical properties in solid state were characterized by differential scanning calorimeter (DSC), powder X-ray diffraction (PXRD), Fourier transform infrared spectrometry (FT-IR) and scanning electron microscopy. No endothermic and characteristic diffraction peaks corresponding to CA were observed for the solid dispersions in DSC and PXRD. FTIR analysis demonstrated the presence of intermolecular hydrogen bonds between CA and HPMC 2910/PVP K-30 in solid dispersions, resulting in the formation of amorphous or non-crystalline CA. Dissolution studies indicated that the dissolution rates were remarkably increased in solid dispersions compared with those in the physical mixture and drug alone. In conclusion, an amorphous or non-crystalline CA solid dispersion prepared using SEDS could be very useful for the formulation of solid dosage forms.

Introduction

In the pharmaceutical literature, solid dispersion systems in which the drug is dispersed in solid water-soluble matrices either molecularly or as fine particles have shown promising results in increasing the bioavailability of poorly water-soluble drugs, and the amorphous state of the drug is often preferred in solid dispersions since it shows a greater solubility and dissolution rate in comparison to the crystalline materials (Leuner & Dressman 2000; Craig 2001). Water-soluble carriers such as high molecular weight polyethylene glycols, polyvinylpyrrolidones (PVP) and hydroxypropylmethylcellulose (HPMC) have been widely used for solid dispersions (Serajuddin 1999).

A number of techniques have been developed for the preparation of solid dispersions, including milling, spray-drying, freeze-drying and solvent evaporation (Chiou & Riegelman 1971). The major disadvantages of these conventional techniques are the thermal and chemical degradation of products due to high temperatures, high energy requirements, solvent residues and broad particle size distributions (PSDs). However, supercritical fluid (SCF) technology provides a novel alternative for formulating co-precipitates that may be smaller in particles size, lower in residual organic solvent with better flowability and that overcome some of the problems faced in conventional methods (Beach et al 1999; Moneghini et al 2001). Supercritical carbon dioxide (SC-CO_2) exists as a single fluid phase above its critical temperature (T_c) and pressure (P_c). Carbon dioxide is currently the most commonly used supercritical fluid because of its low critical temperature and pressure ($T_c = 31.0°C$, $P_c = 7.38$ MPa). Apart from being non-toxic, non-flammable and inexpensive, the low critical temperature of carbon dioxide makes it attractive for processing heat-labile pharmaceuticals.

The particle formation processes involving SC-CO_2 that are most often referred to are the rapid expansion of supercritical solutions (Matson et al 1987; Turk et al 2002; Gosselin et al 2003) and the supercritical antisolvent system (SAS) (Reverchon et al 1998; Chattopadhyay & Gupta 2001; Yeo et al 2003). Based on the principle of SAS, a novel technique called solution enhanced dispersion by supercritical fluids (SEDS) has been developed (Hanna & York 1993). In this process, the SC-CO_2 is used both for

National Research Laboratory of Pharmaceutical Technology, College of Pharmacy, Chungnam National University, 220 Gung-dong, Yuseong-gu, Daejeon 305-764, Korea

Seoung Wook Jun, Min-Soo Kim, Guk Hyun Jo, Sibeum Lee, Jong Soo Woo, Jeong-Sook Park, Sung-Joo Hwang

Correspondence: Sung-Joo Hwang, National Research Laboratory of Pharmaceutical Technology, College of Pharmacy, Chungnam National University, 220 Gung-dong, Yuseong-gu, Daejeon 305-764, Korea.
E-mail: sjhwang@cnu.ac.kr

Acknowledgements and funding: This study was supported by a grant from the National Research Laboratory Program in the series MOST-NRDP (Contact number MI-0302-00-0016) in the Ministry of Science and Technology, Korea and also partly supported by a grant from the Program for Regional Scientists (contact number R05-2003-000-100.85), Korea Science and Engineering Foundation, Korea.

its chemical properties and as a 'spray enhancer' using a mechanical effect in order to achieve smaller droplet size and intense mixing of SC-CO_2 and solution for increased transfer rates; a nozzle with two-flow passages allows the introduction of SC-CO_2 and a solution of active substances into the particle precipitation vessel where pressure and temperature are controlled. The high velocity of the SC-CO_2 breaks up the solution into very small droplets. Moreover, the conditions are set up so that the SC-CO_2 can extract the solvent from the solution at the same time as it meets and disperses the solution (Palakodaty et al 1998; Juppo et al 2003). SCF technology has also been used for processing diverse materials, including low molecular weight substances, proteins and polymers (Moshashaee et al 2000; Reverchon et al 2002).

Cefuroxime is the first commercially available second-generation cephalosporin to be widely used in therapy. It is a semi-synthetic cephalosporin obtained from the 7-cephalosporanic acid nucleus of cephalosporin C (Powell et al 1991; Dellamonica 1994). Cefuroxime axetil (CA) is the acetoxyethyl ester of the cephalosporin cefuroxime. Since CA is slightly soluble in water and can form a thicker gel on contact with an aqueous medium, it shows poor dissolution and subsequently low bioavailability in the gastrointestinal tract (Woo & Chang 2000; Woo et al 2002).

In this study, CA solid dispersions with HPMC 2910/PVP K-30 were prepared using SEDS in an effort to increase the dissolution rate of the drug and subsequently its bioavailability. Their physicochemical properties in the solid state were characterized by differential scanning calorimetry (DSC), powder X-ray diffraction (PXRD), Fourier transform infrared spectroscopy (FT-IR) and scanning electron microscopy (SEM). In addition, equilibrium solubility and dissolution studies were carried out.

Materials and Methods

Materials

CA as the model drug was kindly supplied by Hanmi Pharmaceutical Co. Ltd (Korea). HPMC 2910 (Pharmacoat 606) and PVP K-30 (Kollidon K-30) were purchased from BASF (Ludwigshafen, Germany) and Shinetsu Chemical Co. Ltd (Japan), respectively. Carbon dioxide with high purity of 99.99% was supplied from Myungsin General Gas Co. Ltd (Korea). All other chemicals were of reagent grade and used without further purification.

Solution enhanced dispersion by supercritical fluids

SEDS was performed using experimental equipment described previously (Won et al 2005). SC-CO_2 was pumped to the top of the particle precipitation vessel (internal volume 847.8 cm^3; internal diameter 9 cm; length 30 cm) through the inner capillary of the two-flow ultrasonic spray nozzle (Sonimist HSS-600–1, Misonix Inc., NY) by ISCO syringe pump (Model 260D, maximum operation pressure 80 MPa, maximum liquid flow rate 86 mL min^{-1}). Once the particle precipitation vessel reached steady state (above critical temperature and pressure), the drug/water-soluble polymeric carrier solution was introduced into the particle precipitation vessel by an HPLC liquid pump (NP-AX-15, Nihon Seimitsu Kagaku Co. Ltd, Japan; maximum operating pressure 80 MPa, liquid flow rate 0.01–9.99 mL min^{-1}) through the two-flow ultrasonic spray nozzle. Meanwhile, the SC-CO_2 continued to flow through the vessel to maintain the steady state; the precipitates were collected on the walls and bottom of the vessel. The residual solvent (SC-CO_2 and organic solvent) was drained out of the particle precipitation vessel by the backpressure regulator (Tescom, model 26-1723-24-194). After the spraying of drug/water-soluble polymeric solution into the particle precipitation vessel was completed, additional SC-CO_2 continued to flow into the vessel for a further 60 min to remove residual solvent from the precipitated particles. It was then slowly depressurized to atmospheric pressure.

Preparation of solid dispersions and physical mixture with HPMC 2910/PVP K-30

The CA solid dispersions with HPMC 2910/PVP K-30 were prepared using SEDS at various ratios of drug/water-soluble polymeric carriers (60:40, 50:50 and 40:60 w/w %) as described above. Briefly, the drug/water-soluble polymeric carrier solutions (2.5%, w/w) were prepared by dissolving CA and HPMC 2910/PVP K-30 with a minimum volume of dichloromethane and ethanol (6:4 w/w %) and then sprayed into the particle precipitation vessel through a two-flow ultrasonic spray nozzle with CO_2. When the drug/water-soluble polymeric carrier solutions expanded into SC-CO_2, particles were precipitated in the particle precipitation vessel. During particle precipitation, the operating pressure and temperature were fixed at 10 MPa and 45°C. In addition, the flow rates of CO_2 and the drug/water-soluble polymeric carrier solution were 30 and 0.5 mL min^{-1}, respectively. The precipitated particles were collected on the walls and bottom of the particle precipitation vessel and then stored in a desiccator at room temperature. Physical mixtures were also prepared by mixing CA with HPMC 2910/ PVP K-30 at the same ratio (60:40, 50:50 and 40:60 w/w %) in a mortar and pestle until homogeneous mixtures were obtained. All of the samples were passed through a 250-μm sieve (mesh size 60) and then stored in a desiccator at room temperature.

Differential scanning calorimetry

Prior to DSC analysis, a baseline was obtained that was used as a background. DSC analyses of samples were carried out on DSC S-650 (Scinco Co. Ltd, Korea). Temperature and enthalpy were calibrated with the standard materials indium (melting point 156.6°C) and zinc (melting point 419.5°C) at a heating rate of 5°C min^{-1}. Samples (3–4 mg) were accurately weighed and sealed in aluminium pans and heated at a rate of 5°C min^{-1}. The

measurements were performed in a heating range of 40–200°C under a nitrogen purge. A nitrogen flow rate of 20 mL min^{-1} was used for the DSC run. A chiller unit was used in conjunction with the calorimeter to attain the lower temperatures. All samples were analysed in duplicate.

Powder X-ray diffraction

PXRD patterns of samples were recorded using powder X-ray diffractrometry (Generator Rigaku, D/max-IIIC; Goniometer θ/θ goniometer), with an Ni filtered Cu-Kα line as the source of radiation, which was operated at a voltage of 40 kV and a current of 45 mA. Each sample was placed in the cavity of an aluminium sample holder flattened with a glass slide to present a good surface texture and inserted into the sample holder. In order to measure the powder pattern, the sample holder and detector were moved in a circular path to determine the angles of scattered radiation and to reduce preferred sample orientation. All samples were measured in the 2θ angle range between 0 and 50°C with a scan rate of 3°C min^{-1} and a step size of 0.01°C. All samples were analysed in duplicate.

Fourier transform infrared spectroscopy

FT-IR spectra were obtained using an ATR FT-IR spectrometer (Travel IR, USA) equipped with a DTGS detector. A resolution of 2 cm^{-1} was used and 64 scans were co-added for each spectrum over a frequency range of 4000–450 cm^{-1}.

Scanning electron microscopy

Particle size and morphology were determined using SEM (Hitachi S-3000N, Japan), operated at an accelerating voltage of 20 kV (filament current 1.75 μA, beam current 30–40 mA, probe current 250 pA). Samples were prepared by mounting approximately 0.5 mg of powder onto a 5×5 mm silicon wafer fixed via graphite tape to an aluminium stub. The powder was then sputter-coated for 40 s at a beam current of 38–42 mA with a 200 Å layer of gold/palladium alloy. Samples were visualized at 30–50 mA at magnifications of 5 or 20–10 k×.

Equilibrium solubility

The equilibrium solubility of pure CA, physical mixtures and solid dispersions with HPMC 2910/PVP K-30 using SEDS at various ratios of drug/water-soluble polymeric carriers were measured in simulated gastric juice (pH 1.2) without pepsin. An excess amount of sample was added to 2 mL of the simulated gastric juice in test-tubes sealed with stoppers. The test-tubes were vortex-mixed for 5 min and then sonicated for 30 min. They were kept in a constant temperature shaking bath maintained at 37 ± 0.5°C until they reached equilibrium (for 24 h). A portion of solution was withdrawn and then filtered with a nylon syringe filter (0.45 μm) and adequately diluted with methanol. The concentration of CA was determined at a wavelength of 278 nm by UV-VIS spectrophotometer (Shimadzu) as described in the US Pharmacopoeia (US Pharmacopoeia XXVI).

Dissolution studies

Dissolution studies were performed according to the rotating paddle method as described in the Cefuroxime Axetil Tablets section of the US Pharmacopoeia (US Pharmacopoeia XXVI). A dissolution apparatus (Vankel VK7000, USA) was employed with a stirring rate of 55 rpm and was maintained 37 ± 0.2°C. The dissolution medium was 900 mL of 0.07 N hydrochloride acids. Accurately weighed CA, physical mixtures and solid dispersions as a powder (300.72 mg as CA) were dispersed in 900 mL of dissolution medium. Samples (5 mL) were collected periodically (3, 5, 10, 15, 20, 30, 45 and 60 min) and then filtered with a 0.45 μm nylon syringe filter and replaced with a fresh dissolution medium. The concentration of CA was determined by UV-VIS spectrophotometry (Shimadzu). The dissolution efficiency (DE) was calculated from the area under the dissolution curves at given times and expressed as a percentage of the area of the rectangle described by 100% dissolution in the same time (Khan 1975). The statistical significance of differences among formulations was estimated by one-way analysis of variance (ANOVA) and the Student–Newman–Keuls test in terms of drug dissolution efficiency, percentage of drug dissolved (PD) at a given time and relative dissolution rate (RDR).

Results and Discussion

Differential scanning calorimetry

Figure 1 shows the representative DSC curves of pure CA, physical mixtures and solid dispersions with HPMC 2910/PVP K-30 prepared using SEDS at 40:60 drug/water-soluble polymeric carriers. Pure CA exhibited two endothermic bands around 125 and 181°C, indicating that CA as a model drug existed as a mixture of the crystalline form K and the substantially amorphous form A^{II}. It is well known that CA exists in three polymorphs: one crystalline form K with a melting point around 181°C, and two substantially amorphous forms, A^{I} with a low endothermic band around 94°C and A^{II} with a high endothermic band around 125°C (Crisp & Clayton 1985; Crisp et al 1989; Sasinowska et al 1995; Oszczapowicz et al 1995a,b). In addition, the substantially amorphous form A^{I}, with a low endothermic band, showed a 2.4-fold increase in water solubility compared with the crystalline form K (Oszczapowicz et al 1995a,b). Broad endothermic bands observed in the DSC curve of HPMC 2910/PVP K-30 are associated with water loss from amorphous HPMC 2910 and PVP K-30. The DSC curves of physical mixtures with HPMC 2910/PVP K-30 also showed two endothermic peaks corresponding to pure CA, indicating the presence of crystallinity. In contrast, no endothermic peaks corresponding to pure CA were observed in solid dispersions prepared using SEDS. A number of studies have shown that PVP used in solid dispersions can inhibit the crystallization of drugs, resulting in the formation of the amorphous form of the drug in solid dispersions (Sekikawa et al 1978; Yoshioka et al 1995; Van den Mooter et al 1998, 2001; Matsumoto & Zografi 1999).

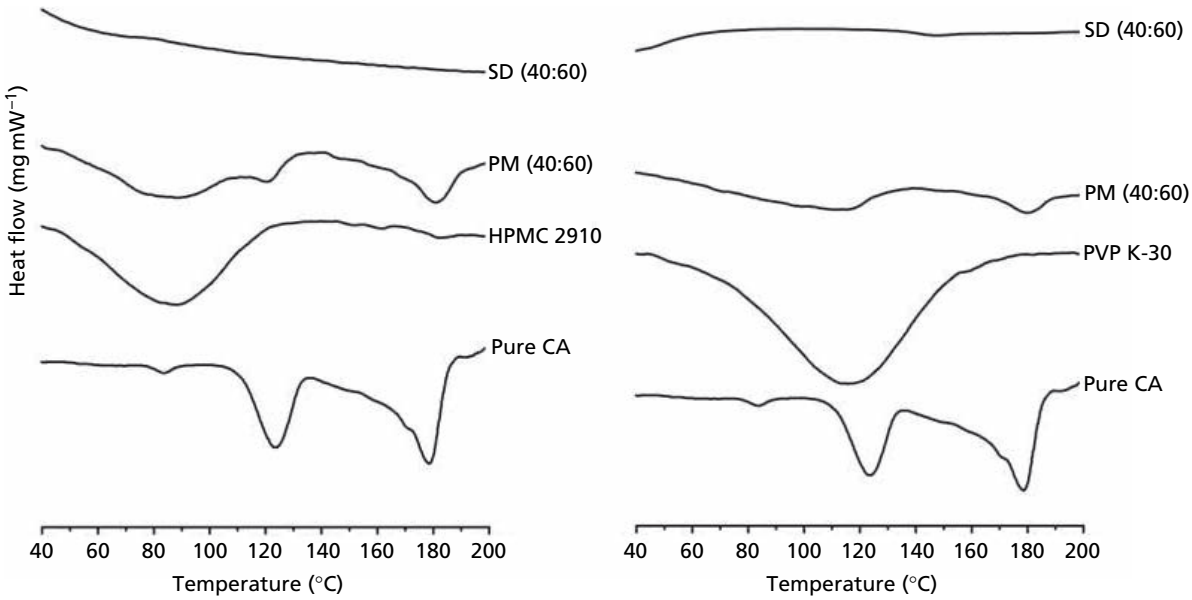

Figure 1 Representative DSC curves of pure CA, physical mixture (PM) and solid dispersion (SD) with HPMC 2910 (left)/PVP K-30 (right) at 40:60 of drug/water-soluble polymeric carriers, respectively, after SEDS.

The crystallization inhibition by HPMC 2910/PVP K-30 is often due to interactions, such as hydrogen bonding, between a drug and water-soluble polymeric carriers. DSC analysis therefore suggests that CA might be presented in completely amorphous or non-crystalline form within solid dispersions owing to crystallization inhibition of the drug by HPMC 2910/PVP K-30.

Powder X-ray diffractometry

Pure CA, physical mixtures and solid dispersions with HPMC 2910/PVP K-30 prepared using SEDS at various ratios of drug/water-soluble polymeric carriers were also investigated by PXRD. The PXRD patterns of pure CA, physical mixtures and solid dispersions prepared using SEDS process are shown in Figure 2. The PXRD patterns

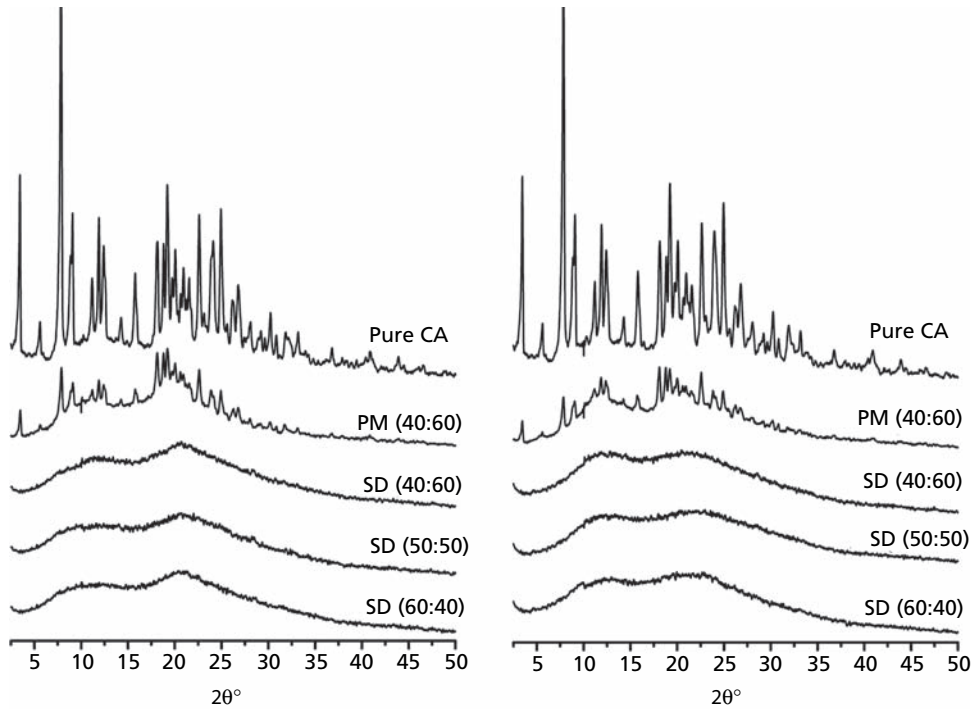

Figure 2 Power X-ray diffraction patterns of pure CA, physical mixture (PM) and solid dispersions (SD) with HPMC 2910 (left)/PVP K-30 (right) at various ratios of drug/water-soluble polymeric carriers, respectively, after SEDS.

of CA and their physical mixtures show characteristic high-intensity diffraction peaks at 2θ values of 3.45°, 5.60°, 7.84°, 9.07°, 11.92°, 15.81°, 19.23°, 22.64° and 24.95°, indicating that CA is highly crystalline in nature, as indicated by numerous characteristic diffraction peaks, and still present in crystalline form within physical mixtures. On the other hand, the PXRD patterns of solid dispersions prepared using SEDS were completely different from those of pure CA and their physical mixtures. The PXRD spectra of all solid dispersions did not show any characteristic diffraction peaks corresponding to pure CA, confirming that CA is present in amorphous or non-crystalline form within solid dispersions. From these results, all solid dispersions prepared using SEDS exhibited no crystallinity, indicating the absence of sharp diffraction peaks corresponding to CA. It is evident that there is probably an important interaction, such as hydrogen bonding, between pure CA and HPMC 2910/PVP K-30 during the preparation of solid dispersions using SEDS.

FT-IR spectroscopy

FT-IR studies were carried out to investigate the possible interactions between pure CA and HPMC 2910/PVP K-30 within solid dispersions. Figure 3 shows the FT-IR spectra of pure CA, HPMC 2910, PVP K-30, physical mixtures and solid dispersions with HPMC 2910/PVP K-30 prepared using SEDS at various ratios of drug/water-soluble polymeric carriers. In case of HPMC 2910 and PVP K-30, absorption bands were observed at 3452 cm^{-1} (O–H stretching), 2898 cm^{-1} (C–H stretching), 1052 cm^{-1} (C–O–C) and 2946 cm^{-1} (C–H stretching) and 1660 cm^{-1} (C=O), respectively. A very broad absorption band observed at 3435 cm^{-1} in the FT-IR spectrum of PVP K-30 was attributed to the presence of water and confirmed by DSC analysis. In the FT-IR spectra of pure CA, two separate absorption bands were observed at 3305 and 3270 cm^{-1} for N–H stretching (primary amide), and C=O stretching of β-lactam, ester, carbamyl and amide groups was observed at 1770 and 1746 $cm^{-1}$and 1710 and 1650 cm^{-1}, respectively. These absorption bands were also observed for the physical mixtures with HPMC 2910/ PVP K-30 with the same absorbance, suggesting that there is no important interaction between pure CA and HPMC 2910/PVP K-30 in physical mixtures and CA maintains its crystallinity, as observed in DSC and PXRD analysis. In contrast, absorption bands corresponding to the symmetrical and asymmetrical N–H stretching vibrations of primary amide groups of CA at 3410 and 3270 cm^{-1} were not observed, and the C=O stretching bands observed at 1770, 1746, 1710 and 1650 cm^{-1} were broader in the FT-IR spectra of solid dispersions with HPMC 2910/PVP K-30, respectively. Taylor & Zografi (1997) reported that PVP has two functional groups, i.e. =N– and C=O, that can potentially form hydrogen bonds with the drug. However, steric hindrance precludes the involvement of nitrogen atoms in intermolecular interactions, thus making the carbonyl group more favourable for hydrogen bonding. These results suggest that the N–H and C=O functional groups of CA interact with the O–H of HPMC 2910 and the C=O of PVP K-30 at the

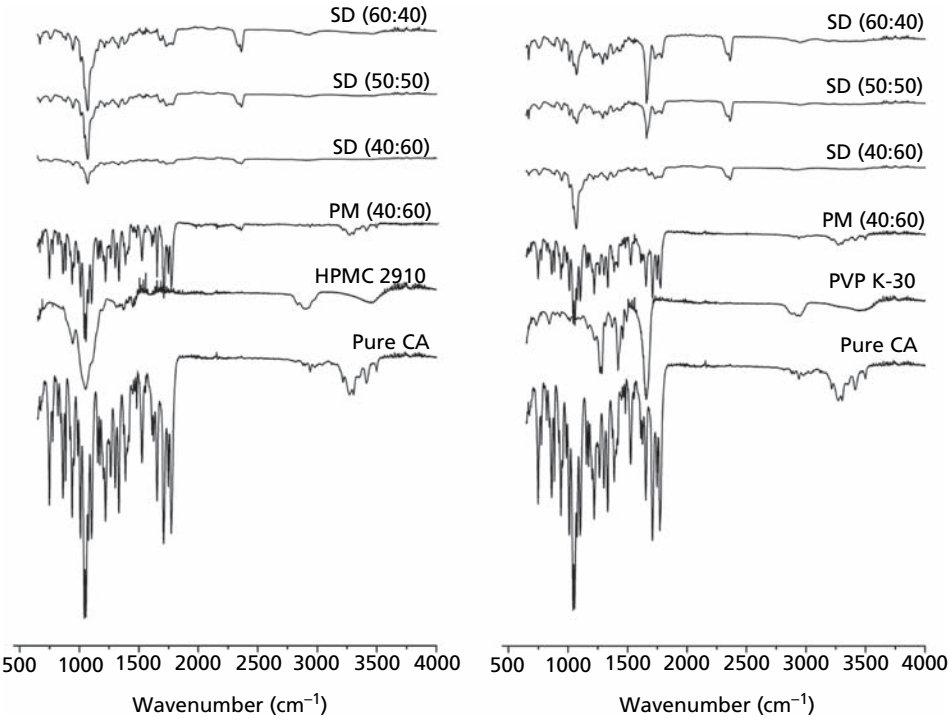

Figure 3 FT-IR spectra of pure CA, physical mixture (PM) and solid dispersions (SD) with HPMC 2910 (left)/PVP K-30 (right) at various ratios of drug/water-soluble polymeric carriers, respectively, after SEDS.

molecular level in solid dispersions prepared using SEDS, resulting in the formation of amorphous or non-crystalline forms of CA.

Equilibrium solubility

Table 1 shows the equilibrium solubility of pure CA, physical mixtures and solid dispersions with HPMC 2910/PVP K-30 prepared using SEDS at various ratios of the drug/water-soluble polymeric carrier. Pure CA exhibited an equilibrium solubility of $0.4 \pm 0.13\,mg\,mL^{-1}$, while the equilibrium solubilities of solid dispersions with HPMC 2910/PVP K-30 prepared with 40:60 drug/water-soluble polymeric carriers were 2.7 ± 0.30 and $3.2 \pm 0.22\,mg\,mL^{-1}$, respectively. All solid dispersions prepared using SEDS showed approximately 5- or 7-fold increases and their physical mixtures were also increased 2- or 3-fold in equilibrium solubility compared with pure CA as a model drug. Moreover, equilibrium solubility was increased with respect to the amount of water-soluble polymeric carriers used, despite marginal differences in equilibrium solubility among the solid dispersions prepared. The formation of amorphous or non-crystalline forms within solid dispersions by adding water-soluble polymeric carriers such as HPMC 2910/PVP K-30 may account for the improvement in equilibrium solubility of the drug from solid dispersions compared with the drug alone and physical mixtures. Better equilibrium solubility from solid dispersions with PVP K-30 may be attributed to a stronger interaction between CA and PVP K-30 than for HPMC 2910. In addition, as presented in Figure 4, pure CA was presented as irregular and flaky particles (size range *c.* 5–10 μm) whereas all solid dispersions prepared using SEDS at various ratios were presented as regular and spherical particles (size range *c.* 200–300 nm) with narrow PSDs.

Dissolution studies

The mean dissolution profiles of a solid dispersion prepared using SEDS at a 40:60 ratio of drug/water soluble polymeric carriers were measured and compared to those of pure CA and physical mixtures (Figure 5). Table 2 shows the mean dissolution profiles of pure CA, physical mixtures and solid dispersions for each water-soluble polymeric carrier, in terms of PD after 10 and 30 min, dissolution efficiency at 60 min (DE_{60}) and RDR at 5 min. The results in Table 2 show that the dissolution of drug from solid dispersions with HPMC 2910/PVP K-30 prepared using SEDS was significantly improved compared to pure CA. The CA alone resulted in $27.5 \pm 1.90\%$ of drug dissolved at 30 min, while solid dispersions with HPMC 2910/PVP K-30 resulted in 97.2 ± 1.23 and $98.8 \pm 1.10\%$, respectively. All solid dispersions exhibited faster dissolution rates than CA with approximately 3.6- and 9-fold increases in terms of both DE_{60} and RDR. The analysis of variance shows that there are significant differences among the formulations ($F_{4,25} = 4293.714$, $P < 0.001$) and the DE_{60} increased in the following order: pure CA < physical mixture with HPMC 2910 < physical mixture with PVP K-30 < solid dispersions with HPMC606/PVP K-30, ranked by the Student–Newman–Keuls test. Unlike equilibrium solubility, there was no significant difference between solid dispersions with HPMC 2910 and PVP K-30 in the dissolution study. For poorly water-soluble drugs it is well known that even a small increase in dissolution will result in a large increase in bioavailability since the bioavailability of a poorly water-soluble drug is often limited by dissolution rate (Lobenberg & Amidon 2000). There are numerous publications to improve the dissolution of a drug and particularly its bioavailability via solid dispersions (Simonelli et al 1976; Sekikawa et al 1979; Moneghini et al 2001). Typical mechanisms for the improvement of dissolution characteristics of drugs by solid dispersion are a reduction in particle size, the absence of crystallinity due to the formation of amorphous forms and improved wettability (Leuner & Dressman 2000). Based on the results from our study, the higher dissolution rate of CA from solid dispersions was probably attributed to the formation of amorphous or non-crystalline forms due to intermolecular hydrogen bonds, resulting from the crystallization inhibition by HPMC 2910/PVP K-30, the increased wettability and reduction in particle size, resulting in an increased surface area available for dissolution.

Table 1 Composition and equilibrium solubility of pure CA, physical mixtures and solid dispersions prepared using SEDS at various ratios of drug/water-soluble polymeric carriers (n = 3)

Composition of drug/water-soluble polymeric carriers (ratio)	Equilibrium solubility ($mg\,mL^{-1}$)	
	Solid dispersions	Physical mixture
Pure CA	0.4 ± 0.13	–
CA:HPMC 2910 (60:40)	2.4 ± 0.19	1.2 ± 0.20
CA:HPMC 2910 (50:50)	2.7 ± 0.15	1.0 ± 0.14
CA:HPMC 2910 (40:60)	2.7 ± 0.30	0.8 ± 0.20
CA:PVP K-30 (60:40)	2.9 ± 0.24	0.8 ± 0.32
CA:PVP K-30 (50:50)	3.1 ± 0.18	0.8 ± 0.10
CA:PVP K-30 (40:60)	3.2 ± 0.22	0.9 ± 0.16

Conclusions

In this study, SEDS has been applied to prepare CA solid dispersions with HPMC 2910/PVP K-30. All solid dispersions exhibited faster dissolution rates than those of physical mixtures and drug alone. FT-IR analysis indicated that CA was present in amorphous or non-crystalline forms within solid dispersions and was found to interact with HPMC 2910 and PVP K-30 by hydrogen bonding. The improved equilibrium solubility and dissolution are attributable to the formation of amor-

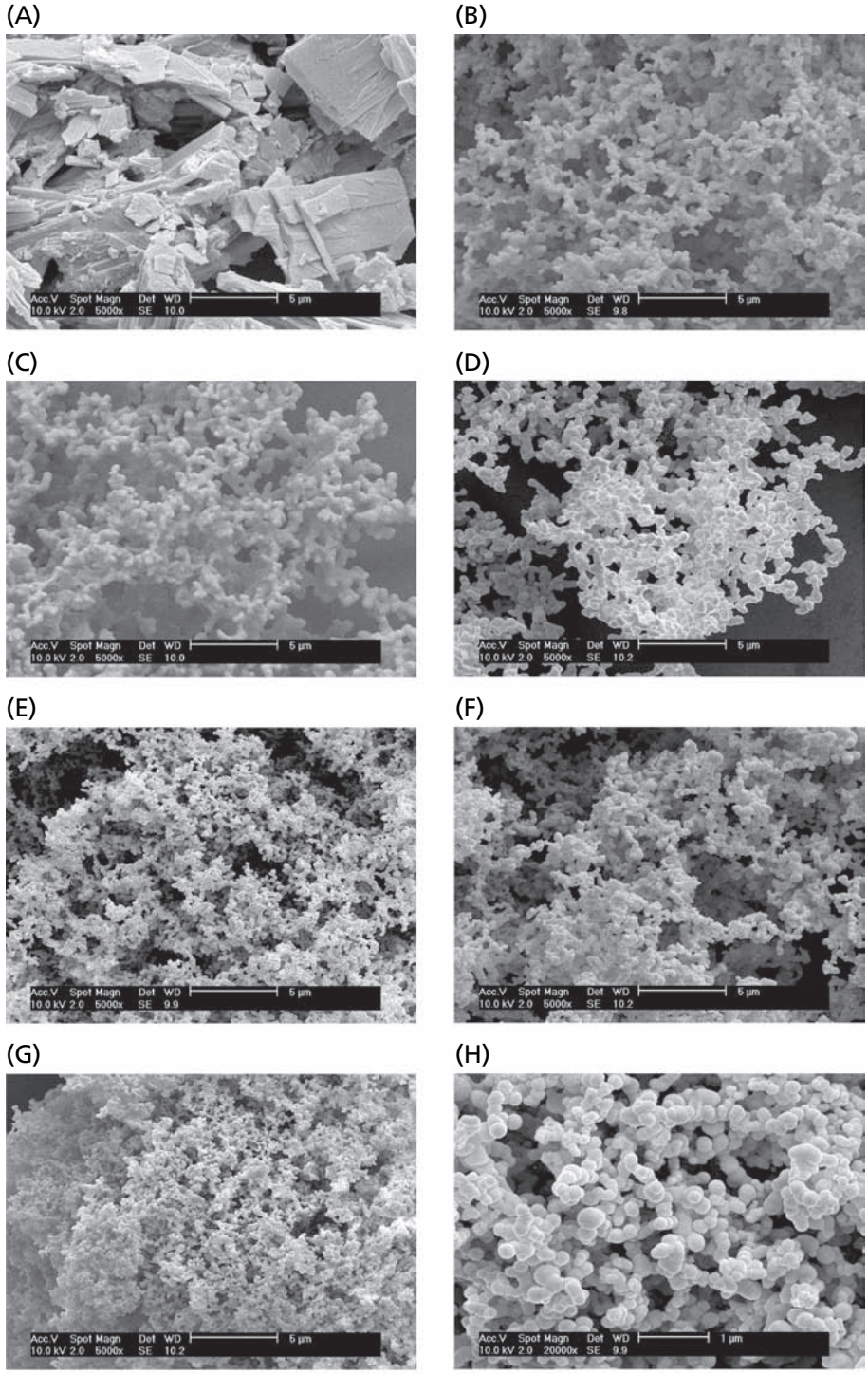

Figure 4 SEM photomicrographs of pure CA (A) and solid dispersions with HPMC 2910 (B, C, D)/PVP K-30 (E, F, G, H) prepared using SEDS at 40:60, 50:50, 60:40 (w/w %) of drug/water-soluble polymeric carriers, respectively (× 5000 and × 20 000).

phous or non-crystalline forms of CA within solid dispersions due to specific interactions between the drug and HPMC 2910/PVP K-30 during SEDS, resulting in crystallization inhibition by HPMC 2910/PVP K-30, increased wettability and a reduction in particle size. These CA solid dispersions prepared using SEDS would therefore be very useful for the formulation of solid dosage forms.

Table 2 Dissolution efficiency at 60 min, percentage drug dissolved at 10 and 30 min, and relative dissolution rate of pure CA, physical mixtures (PM) and solid dispersions (SD) prepared using SEDS at 40:60 of drug/water-soluble polymeric carriers (n = 6)

Sample	% drug dissolved (PD)		DE_{60}[a]	RDR[b] (5 min)
	10 min	30 min		
Pure CA	13.5 ± 0.60	27.5 ± 1.90	25.6 ± 0.40	1
PM with HPMC 2910	28.3 ± 1.48	52.4 ± 2.20	47.5 ± 1.65	2.3
PM with PVP K-30	32.8 ± 0.74	59.7 ± 0.63	54.1 ± 0.80	2.9
SD with HPMC 2910	85.5 ± 2.28	97.2 ± 1.23	91.0 ± 1.06	9.1
SD with PVP K-30	88.2 ± 2.05	98.8 ± 1.10	91.6 ± 1.07	9.4

[a]Calculated from the area under the dissolution curve at 60 min and expressed as the percentage of the area of the rectangle described by 100% dissolution in the same time.
[b]Ratio between amount of drug dissolved from physical mixtures/solid dispersions and that dissolved from pure CA at 5 min.

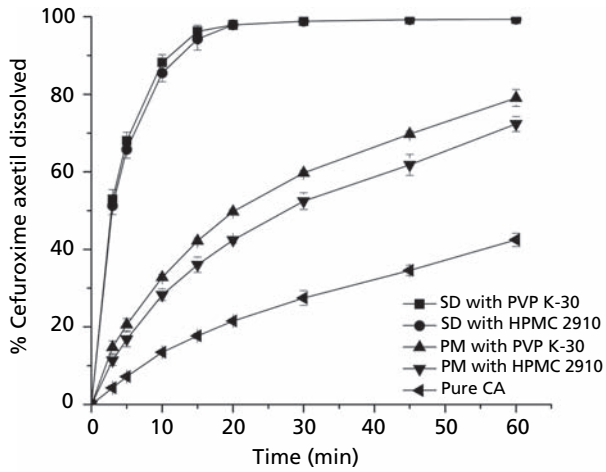

Figure 5 Mean dissolution profiles of pure CA, physical mixtures (PM) and solid dispersions (SD) using SEDS prepared at 40:60 of drug/water-soluble polymeric carriers, respectively (n = 6).

References

Beach, S., Latham, D., Sidgwick, C., Hanna, M., York, P. (1999) Control of the physical form of salmeterol xinafoate. *Org. Process Res. Dev.* **3**: 370–376

Chattopadhyay, P., Gupta, R. B. (2001) Production of griseofulvin nanoparticles using supercritical CO_2 antisolvent with enhanced mass transfer. *Int. J. Pharm.* **228**: 19–31

Chiou, W. L., Riegelman, S. (1971) Pharmaceutical applications of solid dispersion systems. *J. Pharm. Sci.* **60**: 1281–1302

Craig, D. Q. M. (2001) The mechanisms of drug release from solid dispersions in water-soluble polymers. *Int. J. Pharm.* **231**: 131–144

Crisp, H. A., Clayton, J. C. (1985) Amorphous form of cefuroxime ester, US Patent 4 562 181

Crisp, H. A., Clayton, J. C., Elliott, L. G., Wilson, E. M. (1989) Preparation of a highly pure, substantially amorphous form of cefuroxime axetil, US Patent 4 820 833

Dellamonica, P. (1994) Cefuroxime axetil. *Int. J. Antimicrob. Agents* **4**: 23–36

Gosselin, P. M., Thibert, R., Preda, M., McMullen, D. N. (2003) Polymorphic properties of micronized carbamazepine produced by RESS. *Int. J. Pharm.* **252**: 225–233

Hanna, M., York, P. (1993) Method and apparatus for the formation of particles, European Patent 93 13642 2

Juppo, A. M., Boissier, C., Khoo, C. (2003) Evaluation of solid dispersion particles prepared with SEDS. *Int. J. Pharm.* **250**: 385–401

Khan, K. A. (1975) The concept of dissolution efficiency. *J. Pharm. Pharmacol.* **27**: 48–49

Leuner, G., Dressman, J. (2000) Improving drug solubility for oral delivery using solid dispersions. *Eur. J. Pharm. Biopharm.* **50**: 47–60

Lobenberg, R., Amidon, G. L. (2000) Modern bioavailability, bioequivalence and biopharmaceutics classification system. New scientific approaches to international regulatory standards. *Eur. J. Pharm. Biopharm.* **50**: 3–12

Matson, D. W., Fulton, J. L., Petersen, R. C., Smith, F. D. (1987) Rapid expansion of supercritical fluid solutions: solute formation of powders, thin films, and fibers. *Ind. Eng. Chem. Res.* **26**: 2298–2306

Matsumoto, T., Zografi, G. (1999) Physical properties of solid molecular dispersions of indomethacin with poly(vinylpyrrolidone) and poly(vinylpyrrolidone-co-vinylacetate) in relation to indomethacin crystallization. *Pharm. Res.* **16**: 1722–1728

Moneghini, M., Kikic, I., Voinovich, K., Perissutti, B., Filipovic-Grcic, J. (2001) Processing of carbamazepine-PEG 4000 solid dispersions with supercritical carbon dioxide: preparation, characterization, and in vitro dissolution. *Int. J. Pharm.* **222**: 129–138

Moshashaee, S., Bisrat, M., Forbes, R. T., Nyqvist, H., York, P. (2000) Supercritical fluid processing of proteins. I: lysozyme precipitation from organic solution. *Eur. J. Pharm. Sci.* **11**: 239–245

Oszczapowicz, I., Malafiej, E., Szelachowska, M., Horoszewicz-Malafiej, A., Kuklewicz, C., Sieranska, E., Denys, A., Niedworok, J. (1995a) Esters of cephalosporins, Part II. Differences in the properties of various forms of the 1-acetoxyethyl ester of cefuroxime. *Acta. Polon. Pharm. Drug Res.* **52**: 397–401

Oszczapowicz, I., Malafiej, E., Horoszewicz-Malafiej, A., Szelachowska, M., Kuklewicz, C., Sieranska, E. (1995b) Esters of cephalosporins, Part III. Separation and properties of the R and S isomers of the 1-acetoxyethyl ester of cefuroxime. *Acta. Polon. Pharm. Drug Res.* **52**: 471–476

Palakodaty, S., York, P., Pritchard, J. (1998) Supercritical fluid processing of materials from aqueous solutions: the application of SEDS to lactose as a model substance. *Pharm. Res.* **15**: 1835–1843

Powell, D. A, James, N. C., Ossi, M. J., Nahata, M. C., Donn, K. H. (1991) Pharmacokinetics of cefuroxime axetil suspension in infants and children. *Antimicrob. Agents. Chemother.* **35**: 2042–2045

Reverchon, E., Della Porta, G., Trolio, A. D., Pace, S. (1998) Supercritical antisolvent precipitation of nanoparticles of superconductor precursors. *Ind. Eng. Chem. Res.* **37**: 952–958

Reverchon, E., De Macro, I., Della Porta, G. (2002) Tailoring of nano- and micro-particles of some superconductor precursors by supercritical antisolvent precipitation. *J. Supercrit. Fluids* **23**: 81–87

Sasinowska, M., Winiewska, I., Gumulka, W., Oszczapowicz, I., Szelachowska, M., Interewiez, B. (1995) Esters of cephalosporins, Part I. Permeability of cefuroxime liberated from its 1-acetoxyethyl ester through biological membranes; influence of the form and size of the ester particles. *Acta. Polon. Pharm. Drug Res.* **52**: 397–401

Sekikawa, H., Nakano, M., Arita, T. (1978) Inhibitory effect of polyvinylpyrrolidone on the crystallization of drugs. *Chem. Pharm. Bull.* **26**: 118–126

Sekikawa, H., Nakano, M., Arita, T. (1979) Dissolution mechanisms of drug-polyvinylpyrrolidone coprecipitates in aqueous solution. *Chem. Pharm. Bull.* **27**: 1223–1230

Serajuddin, A. T. M. (1999) Solid dispersion of poorly water-soluble drugs: early promises, subsequent problems, and recent breakthroughs. *J. Pharm. Sci.* **88**: 1058–1066

Simonelli, A. P., Mehta, S. C., Higuchi, W. I. (1976) Dissolution rates of high energy sulfathiazole-povidone coprecipitates. II: characterization of form of drug controlling its dissolution rate via solubility studies. *J. Pharm. Sci.* **65**: 355–361

Taylor, L. S., Zografi, G. (1997) Spectroscopic characterization of interactions between PVP and indomethacin in amorphous molecular dispersions. *Pharm. Res.* **14**: 1691–1698

Turk, M., Hils, P., Helfgen, B., Schaber, K., Martin, H. J., Wahl, M. A. (2002) Micronization of pharmaceutical substances by the Rapid Expansion of Supercritical Solutions (RESS): a promising method to improve bioavailability of poorly soluble pharmaceutical agents. *J. Supercrit. Fluids* **22**: 75–84

US Pharmacopoeia XXVI (USP26) (2002) *Official Monographs: Cefuroxime Axetil Tablets*. US Pharmacopoeia Convention, Rockville, MD, pp 388–389

Van den Mooter, G., Augustijns, P., Blaton, N., Kinget, R. (1998) Physico-chemical characterization of solid dispersions of temazepan with polyethylene glycol 6000 and PVP K30. *Int. J. Pharm.* **164**: 67–80

Van den Mooter, G., Wuyts, M., Blaton, N., Busson, R., Grobet, P., Augustijns, P., Kinget, R. (2001) Physical stabilization of amorphous ketoconazole in solid dispersions with polyvinylpyrrolidone K25. *Eur. J. Pharm. Sci.* **12**: 261–269

Won, D. H., Kim, M. S., Lee, S., Park, J. S., Hwang, S. J. (2005) Improved physicochemical characteristics of felodipine solid dispersion particles by supercritical anti-solvent precipitation process. *Int. J. Pharm.* **301**: 199–208

Woo, J. S., Chang, H. C. (2000) Non-crystalline cefuroxime axetil solid dispersant, process for preparing same and composition for oral administration thereof, US Patent 6 107 290

Woo, J. S., Chang, H. C., Lee, C. H. (2002) Preparation and evaluation of non-crystalline cefuroxime axetil solid dispersion. *J. Kor. Pharm. Sci.* **32**: 73–80

Yeo, S. D., Kim, M. S., Lee, J. C. (2003) Recrystallization of sulfathiazole and chlorpropamide using the supercritical fluid antisolvent process. *J. Supercrit. Fluids* **25**: 143–154

Yoshioka, M., Hancock, B. C., Zografi, G. (1995) Inhibition of indomethacin crystallization in polyvinylpyrrolidone coprecipitates. *J. Pharm. Sci.* **84**: 983–986